Tikrit Journal of Engineering Sciences (2025); 32(2): 1911
DOI: http://doi.org/10.25130/tjes.32.2.23

IRAQI Academic Scientific Journals

ISSN: 1813-162X (Print); 2312-7589 (Online)

Tikrit Journal of Engineering Sciences

available online at: http://www.tj-es.com

TJES Tikrit Journal of Engineering Sciences

Effect of Random Vibration of Rotor Supports with Nano Additives Lubricants

Marwan Abdulrazzaq Salman *[a], Mahmud R. Ismail [b]

[a] Mechanical Engineering Department, Al-Nahrain University, Baghdad, Iraq.
[b] Prosthetics and orthotics Engineering Department, Al-Nahrain University, Baghdad, Iraq.

Keywords:
Rotor dynamics; Flexible rotor; Support; Nanoparticle; CuO; SAE10W-30; Transfer function; Random vibration; Probability.

Highlights:

- The effect of random vibration on rotor support and the nanolubricant with CuO nanoparticle additives.
- White noise excitation was used to simulate stationary ergodic random vibration.
- Mathematical modeling was employed to analyze random responses and evaluate the derivative of the rotor system's transfer function.
- Experiments were conducted with a rotor model and random vibration setup to assess the power spectral density (PSD) and response standard deviations at different conditions.

ARTICLE INFO

Article history:

Received	05 Dec. 2023
Received in revised form	13 Feb. 2024
Accepted	22 May 2024
Final Proofreading	30 Mar. 2025
Available online	31 May 2025

Citation: Salman MA, Ismail MR. **Effect of Random Vibration of Rotor Supports with Nano Additives Lubricants**. *Tikrit Journal of Engineering Sciences* 2025; **32**(2): 1911.
http://doi.org/10.25130/tjes.32.2.23

*Corresponding author:
Marwan Abdulrazzaq Salman
Mechanical Engineering Department, Al-Nahrain University, Baghdad, Iraq.

Abstract: Rotors in various industries often encounter diverse vibrations from their supports, posing potential dangers to system integrity. The present study focuses on the effects of arbitrary stimulation brought on by random vibrations caused by supports, which necessitate statistical methods for evaluation due to their non-deterministic nature. Through white noise excitation, static ergodic random vibrations were simulated, employing mathematical modeling to derive the transfer function equation of the rotor. The investigation extended to examining the impact of copper oxide (CuO) nanoparticles in SAE10W-30 lubricant on random vibrations. Analytical solutions, facilitated by MATLAB software, were employed to solve the governing differential equations, enabling the evaluation of power spectrum density (PSD) and the standard deviation of responses. The experimental investigation of the rotor model reflected the validation of the mathematical model, especially for random vibration analysis. Reductions in standard deviation values suggested that including CuO-NPs caused a more symmetric distribution of responses in the x and y directions, which is intriguing, improving stability and reducing wear due to the effect of CuO nanoparticles on vibration characteristics. The best CuO-NPs weight was 0.0527g at a dynamic viscosity of 0.0593 Pa·s, and the PSD value reached its minimum value. This conclusion implies that using CuO-NPs can decrease the effect of random vibration on the rotor and increase the life span of the rotating machinery system in practical applications.

تأثير الاهتزاز العشوائي لمساند الدوار مع التزييت بإضافات نانوية

مروان عبدالرزاق سلمان[1]، محمود رشيد اسماعيل[2]

[1] قسم هندسة الميكانيكية / جامعة النهرين/ بغداد - العراق.

[2] قسم هندسة الأطراف والمساند والمساند الصناعية/ جامعة النهرين/ بغداد - العراق.

الخلاصة

في التطبيقات الهندسية غالباً ما تتعرض الدوارات الى اهتزازات متنوعة عبر المساند، مما يشكل مخاطر محتملة على سلامة النظام. تُركز هذه الدراسة على تقييم تأثيرات التحفيز العشوائي الناتج عن الاهتزازات العشوائية المسلطة على المساند. مما يستلزم الاستعانة بالأساليب الإحصائية للتقييم بدلا من الاساليب التحليلية المستخدمة في الانواع الاخرى للاهتزاز يتم حث الاهتزاز العشوائي من خلال إستخدام اشارة الضوضاء الابيض، كما تمت محاكات النظام باستخدام النمذجة الرياضية لاشتقاق معادلة الخواص للدوار. وتضمن البحث دراسة تأثير المضافات النانوية لأكسيد النحاس (CuO) لمادة التزييت من نوع SAE10W-30 على الاهتزازات العشوائية. تم حل المعادلات التفاضلية للحركة باستخدام برنامج MATLABمما اتاح تقييم كثافة الطاقة الطيفية (PSD) والانحراف المعياري للاستجابات. أثبتت الدراسة التجريبية باستخدام نموذج لدوار معرض الى الاهتزاز العشوائي صحة النموذج النظري، حيث بينت النتائج تطابقا في تصرفات الاهتزاز العشوائي.كما بينت منحنيات الانحراف المعياري للاستجابة إلى أن استخدام المضاف النانوي CuO-NPs يسبب تحسنا في استجابة الدوار في كلا الاتجاهين y وx، وهو أمر مثير للاهتمام. ويشير هذا التحسن إلى استقرار معزز للنظام وتقليل التآكل، مما يجعل استخدام جسيمات أكسيد النحاس النانوية مفيدا في تطبيقات تخميد الاهتزازات. كما بينت النتائج بان الوزن الأمثل لـ CuO-NPs هو ٠,٠٥٢٧ جم، حيث تصل الزوجة الديناميكية لغاية ٠,٠٥٩٣Pa•s ، مع انخفاض في PSD إلى أدنى مستوى. كما اظهرت النتائج التجريبية أن النموذج النظري يمكن أن يستجيب بشكل معقول لسلوك الاهتزاز العشوائي. تؤكد هذه النتائج على التطبيقات الواعدة لـ CuO-NPs في التخفيف من الآثار الضارة للاهتزازات العشوائية في الأنظمة الدوارة، مما يعزز ادائها على المدى الطويل في ظل ظروف تشغيل متنوعة.

الكلمات الدالة: ديناميكيات الدوار، الدوار المرن، الدعامة، الجسيمات النانوية، أكسيد النحاس، SAE10W-30، دالة النقل، الاهتزاز العشوائي، الاحتمالية.

1.INTRODUCTION

Random vibration is of broad interest in engineering applications. It is often unpredictable oscillations and vibrations experienced by rotating components, such as rotor systems in various machinery and vehicles. Random vibrations have several impacts on rotor systems, leading to efficiency loss or system collapse. Thus, different aspects and sources of random vibrations are being investigated worldwide. For example, reaching the instability threshold of journal-bearing supported rotors caused by self-excited vibrations has been demonstrated to trigger an unbalanced response through numerical simulations and rotor dynamic analysis [1]. Excitations in rotary systems take the form of random vibrations, which can be more effectively modeled using randomly varying forces under realistic operating conditions. The random vibration of rotors is of broad interest in engineering applications. Many researchers have investigated the different aspects and sources of random vibration, for example, the excitation assumed to take the form of random vibration. To study the whirl motion of the Jeffcott rotor, the system was analyzed using kinetic, potential, and dissipation energy. The motion equations were derived using Lagrangian and Simulink Matlab software equations. The response of the two coordinates (Z and Y) and the whirl orbits of the shaft were observed for different mass ratios. The study included a mathematical investigation of the system's stability, which showed stability at 8,000 rpm and a 0.4 mass ratio [2]. Dimentberg et al. explored the impact of uniaxial random excitation on a rotating shaft, revealing two significant effects: rotational amplification of mean square whirl radius and rise in non-excited response with rotation speed, potentially for online rotor stability assessment [3]. Investigating the impact of internal damping on random vibrations in Jeffcott rotor oscillations to random excitation reveals an increase in vibrations as the dynamic instability threshold reaches high speeds. Dimentberg et al. analyzed response PSDs for the coherence function of lateral displacements in two perpendicular directions and provided equations and solutions for calculating instability threshold speed and whirl speed [4]. Driot et al. studied stochastic methods to assess the stability and stationary response of a skew Jeffcott rotor with geometric uncertainty. It uses coordinate transformations and analytical techniques to quantify instability probabilities and statistical moments of forced responses. The study suggests that incorporating stochastic parameters can improve understanding of a rotating machine's sensitivity [5]. Investigates the effect of the damping element on rotor vibration during rubbing, where impacts between the disc and a square hole in the stationary part occur. The results showed that vibration character depends on rotor rotation speed, and applying the correct magnitude current can reduce impact forces [6]. Yaroshevich et al. studied the dynamics of an unbalanced rotor with a vibrating suspension axis and a limited-power asynchronous electric motor. It investigated stationary modes of rotation and the vibrational capture phenomenon, revealing its self-regulation and energy transfer during load oscillations. The results are confirmed through numerical modeling [7]. Nanomaterials have gained significant interest in different research areas in the past few decades due to their unique physical and chemical properties. Nano-additives, for example, are used to improve the

endurance of oil lubricant used in support rotors with journal bearings. In a recent study, copper (II) oxide nanoparticles (CuO-NPs) blended with SAE10W-30 base engine oil were used to enhance piston-liner contact longevity. Interestingly, CuO-NPs, at a concentration of 0.008%, showed excellent anti-wear properties and friction reduction at a speed of 291 RPM and a load of 75.152 N [8]. Another study found that adding CuO-NPs to engine oil improved wear and friction characteristics, with a minimum coefficient of 0.2% and a maximum of 3%. Specifically, CuO-NPs led to better tribological properties and higher viscosity [9]. CuO-NPs are better suited to decrease friction at lower concentrations [10]. Nanoparticle-enhanced lubricating oil with CuO, TiO2, Ag, and Cu in plain journal bearings increased mass coefficients, damping ratios, and fluid-effective stiffness [11]. Kumar et al. used TiO_2 as a nanolubricant oil at different concentrations (0.2%, 0.4%, 0.6%, and 0.8%). The results showed a calorific value and flash point reduction with increasing volume concentrations, suggesting avoiding nanoparticle aggregation to get the best outcomes. A surfactant can help with this performance [12]. Nanofluid lubricant oil has the capability to improve the effectiveness of rotating machinery. Hammza et al. used ANSYS software to analyze the impact of nanofluid lubricant oil on fluid film journal bearings. The results showed that increasing oil fractions reduced dynamic response by 20.4% and 15.5%, and critical speed increased by 25.82% and 16.8%, respectively [13]. The study demonstrated that the TiO_2 additives improve the hydrodynamic journal bearings' performance by improving load-carrying capacity and reducing friction in SAE30 lubricant oil, enhancing performance under high loading conditions [14]. Jaffar et al. explored using TiO_2 and Bi_2O_3 nanoparticles in low-viscosity mineral SN150 base oil to reduce vibrations in hydrodynamic journal bearings. The results showed that Bi2O3 performed well across a wide range of rotational speeds and loads, while TiO2 was more effective at high speeds and loads [15]. The previous researchers studied and focused on analyzing rotating dynamics of different types. Some of them used analytical methods, and some used the analysis in the ANSYS program. These studies frequently fail to include the effect of random vibrations imposed by rotor supports. To close this gap, the present study will examine the impact of random vibration caused by the rotor supports and assess the efficacy of CuO-NPs in mitigating these effects. Using white noise excitation to simulate stationary ergodic random vibration, the study employs mathematical modeling to analyze random responses and evaluate the derivative of the rotor system's transfer function. By incorporating CuO-NPs into SAE10W-30 lubricant, experiments were conducted with a rotor model and random vibration setup to access the PSD and response standard deviations at different conditions. This study is the first to explore this particular area, making this research distinct. By realizing the effects of random vibration excitation from support, this research could contribute to that, aiming to optimize rotating machinery for improved efficiency and longevity.

2.MATHEMATICAL ANALYSIS

In this investigation, the mathematical model according to a Jeffcott rotor was employed to study the random behavior of a flexible rotor, assuming that the stiffness of the shaft is k (Fig. 1). The shaft carries a disc load of mass m and is supported by two journal bearings. These journal bearings possess stiffness values of K_A and K_B and damping values of C_A and C_B. Additionally, the shaft rotations result in two more damping factors: rotating damping (Cr) and non-rotating damping (Cn).

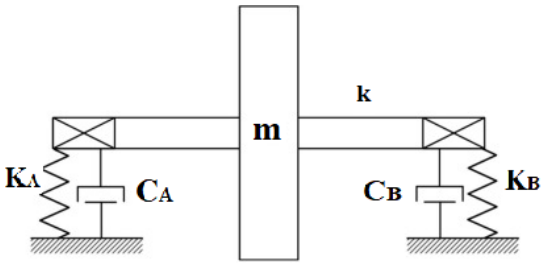

Fig. 1 One Mass on a Flexible Shaft and Flexible Bearings are Characteristics of Jeffcott Rotors.

The equation for the rotor with journal bearing and unbalanced disk is obtained from [16] and expressed in the following matrix form:

$$\begin{bmatrix} m & 0 \\ 0 & m \end{bmatrix}\begin{Bmatrix} \ddot{x}_c \\ \ddot{y}_c \end{Bmatrix} + \begin{bmatrix} c_n + c_r & 0 \\ 0 & c_n + c_r \end{bmatrix}\begin{Bmatrix} \dot{x}_c \\ \dot{y}_c \end{Bmatrix} + \left(\begin{bmatrix} k & 0 \\ 0 & k \end{bmatrix} + \Omega\begin{bmatrix} 0 & c_r \\ -c_r & 0 \end{bmatrix}\right)\begin{Bmatrix} x_c \\ y_c \end{Bmatrix} = \begin{Bmatrix} m\epsilon\Omega^2\cos(\Omega t) \\ m\epsilon\Omega^2\sin(\Omega t) \end{Bmatrix} + \begin{Bmatrix} F_x \\ F_y \end{Bmatrix} \quad (1)$$

2.1.Transfer Function

By assuming zero imbalance forces and support only random vibration, Eq. (1) is reduced to:

$$\begin{bmatrix} m & 0 \\ 0 & m \end{bmatrix}\begin{Bmatrix} \ddot{x}_c \\ \ddot{y}_c \end{Bmatrix} + \begin{bmatrix} c_n + c_r & 0 \\ 0 & c_n + c_r \end{bmatrix}\begin{Bmatrix} \dot{x}_c \\ \dot{y}_c \end{Bmatrix} + \begin{bmatrix} k_x & \Omega c_r \\ -\Omega c_r & k_y \end{bmatrix}\begin{Bmatrix} x_c \\ y_c \end{Bmatrix} = \begin{Bmatrix} F_x \\ F_y \end{Bmatrix} \quad (2)$$

For a harmonic response, Eq. (2) becomes:

$$\begin{bmatrix} -m\omega^2 + i\omega(c_{nx} + c_{rx}) + k_x & \Omega c_{ry} \\ -\Omega c_{rx} & -m\omega^2 + i\omega(c_{ny} + c_{ry}) + k_y \end{bmatrix} \begin{Bmatrix} X_c \\ Y_c \end{Bmatrix} = \begin{Bmatrix} 0 \\ F_y \end{Bmatrix} \quad (3)$$

Using Cramer's Rule to find the response in the x-direction:

$$X_c = \frac{\begin{vmatrix} 0 & \Omega c_{ry} \\ F_y & -m\omega^2 + i\omega(c_{ny} + c_{ry}) + k_y \end{vmatrix}}{\begin{vmatrix} -m\omega^2 + i\omega(c_{nx} + c_{rx}) + k_x & \Omega c_{ry} \\ -\Omega c_{rx} & -m\omega^2 + i\omega(c_{ny} + c_{ry}) + k_y \end{vmatrix}} \quad (4)$$

and in y-direction:

$$Y_c = \frac{\begin{vmatrix} -m\omega^2 + i\omega(c_{nx} + c_{rx}) + k_x & 0 \\ -\Omega c_{rx} & F_y \end{vmatrix}}{\begin{vmatrix} -m\omega^2 + i\omega(c_{nx} + c_{rx}) + k_x & \Omega c_{ry} \\ -\Omega c_{rx} & -m\omega^2 + i\omega(c_{ny} + c_{ry}) + k_y \end{vmatrix}} \quad (5)$$

Two transfer functions are used for the support excitation at the x and y directions:

$$TF_x = \frac{X_c}{F_y} \text{ and } TF_y = \frac{Y_c}{F_y} \quad (6)$$

By separating the real part and imaginary part (also known as $i = -1$), the transfer function becomes:

$$TF_x = \frac{-\Omega c_{ry}}{\begin{bmatrix} -m\omega^2 + i\omega(c_{nx} + c_{rx}) + k_x & \Omega c_{ry} \\ -\Omega c_{rx} & -m\omega^2 + i\omega(c_{ny} + c_{ry}) + k_y \end{bmatrix}} \quad (7)$$

$$TF_y = \frac{-m\omega^2 + i\omega(c_{nx} + c_{rx}) + k_x}{\begin{bmatrix} -m\omega^2 + i\omega(c_{nx} + c_{rx}) + k_x & \Omega c_{ry} \\ -\Omega c_{rx} & -m\omega^2 + i\omega(c_{ny} + c_{ry}) + k_y \end{bmatrix}} \quad (8)$$

By opening the determinate in the dominator,

$$(-m\omega^2 + i\omega c_{rx} + k_x)(-m\omega^2 + i\omega c_{ry} + k_y) + N^2 c_{rx} c_{ry} \quad (9)$$

Solving and re-arranging Eq. (9) and multiplying by complex conjugate to get:

$$TF_x = \frac{-Nc_{ry}(k_x - m\omega^2)(k_y - m\omega^2) + Nc_{ry}\omega^2 c_{rx} c_{ry} - N^3 {c_{ry}}^2 c_{rx} + i\omega N {c_{ry}}^2 (k_x - m\omega^2) + i\omega N c_{rx} c_{ry} (k_y - m\omega^2)}{[(k_x - m\omega^2)(k_y - m\omega^2) - \omega^2 c_{rx} c_{ry} + N^2 c_{rx} c_{ry}]^2 + [\omega c_{ry}(k_x - m\omega^2) + \omega c_{rx}(k_y - m\omega^2)]^2} \quad (10)$$

The real part of Eq. (10) is:

$$= \frac{-Nc_{ry}(k_x - m\omega^2)(k_y - m\omega^2) + Nc_{ry}\omega^2 c_{rx} c_{ry} - N^3 {c_{ry}}^2 c_{rx}}{[(k_x - m\omega^2)(k_y - m\omega^2) - \omega^2 c_{rx} c_{ry} + N^2 c_{rx} c_{ry}]^2 + [\omega c_{ry}(k_x - m\omega^2) + \omega c_{rx}(k_y - m\omega^2)]^2} \quad (11)$$

The Imaginary part of Eq. (10) is:

$$+ \frac{\omega N {c_{ry}}^2 (k_x - m\omega^2) + \omega N c_{rx} c_{ry} (k_y - m\omega^2)}{[(k_x - m\omega^2)(k_y - m\omega^2) - \omega^2 c_{rx} c_{ry} + N^2 c_{rx} c_{ry}]^2 + [\omega c_{ry}(k_x - m\omega^2) + \omega c_{rx}(k_y - m\omega^2)]^2} \quad (12)$$

Following the same steps, the transfer function, multiplied by the complex conjugate, in the y-direction is:

$$TF_y = \frac{(k_x - m\omega^2) + (i\omega c_{rx}) * \{(k_x - m\omega^2)(k_y - m\omega^2) - \omega^2 c_{rx} c_{ry} + N^2 c_{rx} c_{ry} - i\omega c_{ry}(k_x - m\omega^2) - i\omega c_{rx}(k_y - m\omega^2)\}}{[(k_x - m\omega^2)(k_y - m\omega^2) - \omega^2 c_{rx} c_{ry} + N^2 c_{rx} c_{ry}]^2 + [\omega c_{ry}(k_x - m\omega^2) + \omega c_{rx}(k_y - m\omega^2)]^2} \quad (13)$$

The real part of Eq. (13) is:

$$= \frac{(k_x - m\omega^2)^2 (k_y - m\omega^2) - (k_x - m\omega^2)\omega^2 c_{rx} c_{ry} + (k_x - m\omega^2) N^2 c_{rx} c_{ry} \omega^2 c_{rx} c_{ry} (k_x - m\omega^2) + \omega^2 {c_{rx}}^2 (k_y - m\omega^2)}{[(k_x - m\omega^2)(k_y - m\omega^2) - \omega^2 c_{rx} c_{ry} + N^2 c_{rx} c_{ry}]^2 + [\omega c_{ry}(k_x - m\omega^2) + \omega c_{rx}(k_y - m\omega^2)]^2} \quad (14)$$

The imaginary part is:

$$= \frac{\omega c_{ry}(k_x - m\omega^2)^2 - \omega c_{rx}(k_x - m\omega^2)(k_y - m\omega^2) + \omega c_{rx}(k_x - m\omega^2)(k_y - m\omega^2) - \omega^3 {c_{rx}}^2 c_{ry} + \omega N^2 {c_{rx}}^2 c_{ry}}{[(k_x - m\omega^2)(k_y - m\omega^2) - \omega^2 c_{rx} c_{ry} + N^2 c_{rx} c_{ry}]^2 + [\omega c_{ry}(k_x - m\omega^2) + \omega c_{rx}(k_y - m\omega^2)]^2} \quad (15)$$

2.2.Random Vibration Analysis

This analysis assumes that random vibration is stationary and ergodic, which is common for engineering applications. The analysis begins by evaluating the autocorrelation of the random signal. The Autocorrelation Function is denoted as $R_{xx}(\tau)$ and defined as follows:

$$R_{xx}(\tau) = \lim_{T\to\infty} \int_0^T x(t)x(t+\tau)dt \quad (16)$$

The power spectral density (PSD) corresponds to the Fourier transformation of the autocorrelation function:

$$S_{xx}(\omega) = \frac{1}{2\pi}\int_{-\infty}^{\infty} R_{xx}(\omega)\, e^{-j\omega t}d\tau \quad (17)$$

The Random Response ($x(t)$) to Excitation Force ($f(t)$) is simply:

$$x(t) = \int_0^t F(\tau)h(t-\tau)d\tau \quad (18)$$

The PSD of the Response can then be determined as follows:

$$S_{xx}(\omega) = |H(\omega)|^2 \left[\frac{1}{2\pi}\int_{-\infty}^{\infty} R_{ff}(\tau)\, e^{-j\omega t}d\tau\right] \quad (19)$$

OR

$$S_{xx}(\omega) = |H(\omega)|^2 S_{ff}(\omega) \quad (20)$$

$$\bar{x}^2 = \int_{-\infty}^{\infty} S_{xx}(\omega)d\omega \quad (21)$$

2.3.Statistical Analysis of Random Response

In the realm of random vibrations, the notion of time averaging over an extended duration is a recurring concept frequently encountered. The most common notation for this operation is defined by the following equation, in which $x(t)$ is the variable:

$$\overline{x(t)} = \langle x(t)\rangle = \lim_{T\to\infty}\frac{1}{T}\int_0^T x(t)dt \quad (22)$$

The predicted value of x(t), denoted by the notation x(t), is also equal to:

$$E[x(t)] = \lim_{T\to\infty}\frac{1}{T}\int_0^T x(t)dt \quad (23)$$

It is the mean or average value of a quantity sampled repeatedly. The equation provides the predicted value for discrete variables Xi'.

$$E[x] = \lim_{n\to\infty}\frac{1}{n}\sum_{i=1}^{n} x_i \quad (24)$$

The notation $\overline{x^2}$ or $E[x^2(t)]$, used to represent the mean square value, is found by integrating $x^2(t)$ over a time interval T and averaging it out following the formula:

$$E[x^2(t)] = \overline{x^2} = \lim_{T\to\infty}\frac{1}{T}\int_0^T x^2 dt \quad (25)$$

The variance, σ^2, the mean squared value relative to the mean, can be written as:

$$\sigma^2 = \lim_{T\to\infty}\frac{1}{T}\int_0^T (x-\bar{x})^2 dt \quad (26)$$

By extending Eq. (26), it is clear that:

$$\sigma^2 = \overline{x^2} - (\bar{x})^2 \quad (27)$$

The bell-shaped Gaussian distribution, often known as the normal distribution, is symmetric about the mean value [13]:

$$p(x) = \frac{1}{\sigma\sqrt{2\pi}} e^{-\frac{x^2}{2\sigma^2}} \quad (28)$$

The probability of $x(t)$ being between $+\lambda\sigma, -\lambda\sigma$, where λ is any positive number.

λ	Prob$[-\lambda\sigma \le x(t) \le \lambda\sigma]$	Prob$[\lvert x\rvert > \lambda\sigma]$
1	68.3 %	31.7 %
2	95.4 %	4.6 %
3	99.7 %	0.3 %

The absolute value A of the amplitude is an example of a random variable limited to positive values that frequently tends to follow the Rayleigh distribution, which is given by the following equation:

$$p(x) = \frac{A}{\sigma^2} e^{-A^2/2\sigma^2},\ A > 0 \quad (29)$$

λ	P$[> \lambda\sigma]$
0	100 %
1	60.7%
2	13.5 %
3	1.2 %

3.EXPERIMENTAL WORK

An experimental rotor model was designed and fabricated to serve as a universal test rig to validate some rotor-dynamics behaviors related to theoretically investigated parameters, such as the random vibration excitation to the rotor support. Different concentrations of CuO-NPs as lubricant additives were also prepared. The experimental setup consists of a rotor supported by two identical isotropic journal bearings and driven by a three-phase AC motor with a variable speed ranging between 0 and 3360 RPM (Fig. 2). The rotor was connected to the motor using a flexible coupling. The AC motor was connected to the variable frequency drive (AC Drive) to control the angular velocity of the shaft (Fig. 3). Figure 4 represents all the experimental equipment used to test the random vibration on the support. The precise measurements and material specifications are also shown in Table 1. The input and output signals are the only primary categories the measuring system can be divided into, as shown in Figs. 5 and 6. The block schematic for the instruments' random response sections is shown in Fig. 7.

3.1.Nanoparticle Preparation and Journal Lubrication

CuO-NPs were dispersed in SAE 10w-30 oil to analyze journal performance after lubrication. CuO-NPs, which had a spherical structure and a size of 50 nm, were bought from an industrial provider. An analytical balance (with a digital scale) was used to calculate the necessary nanoparticle amount. A mixed suspension of nanoparticles was prepared by dissolving them in ethylene glycol $C_2H_4(OH)_2$ in an ultrasonic bath for five minutes to prevent clumping and allow the particles to disperse rather than settle at the bottom. The oil viscosity was calculated using a rotational viscometer, as shown in Fig. 8.

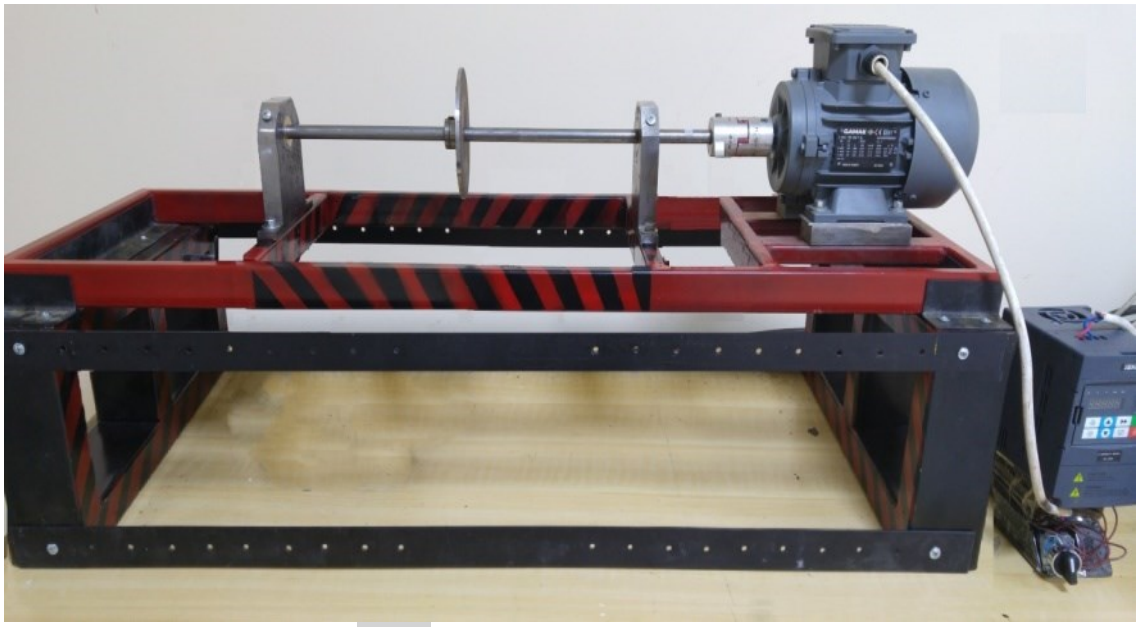

Fig. 2 A Photograph of the Test Rig.

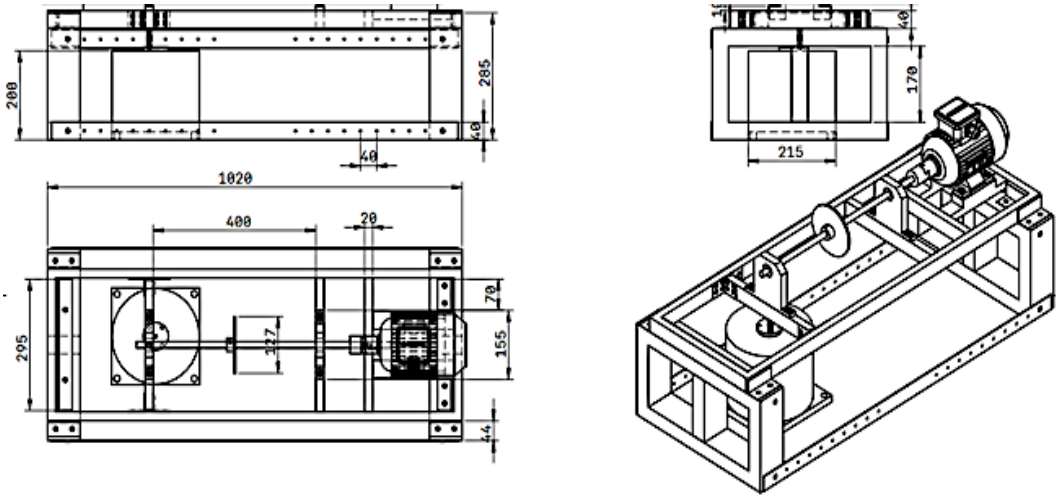

Fig. 3 Schematic Outline Drawing of the Test Rig.

Fig. 4 An Image of the System Used, with a Representation of the Connection of the Shaker with Rotor Support.

Table 1 Mechanical Specifications of the Test Rig Rotor.

Specification	Value	Unit
Shaft length	0.56	m
Shaft diameter	0.014	m
Shaft density	7800	Kg/m^3
Shaft Young's modulus	210×10^9 Carbon Steel CK45	N/m^2
Shaft Poissons Ratio	0.3	-
Support height	0.113	m
Support width	0.95	m
Coupling length	0.067	m
Coupling diameter	0.04	m
Bushing length	0.02	m
Bushing outer diameter	0.03	m
Bushing density	8870	Kg/m^3
Bushing Young's modulus	1.1×10^{11} Copper brass	N/m^2
Shaft to bearing clearance	0.00151	mm
Mass density	7800	Kg/m^3
Mass disk weight	286	g
Mass disk diameter	0.127	m
Mass disk thickness	0.005	m
Distance between supports	0.4	m

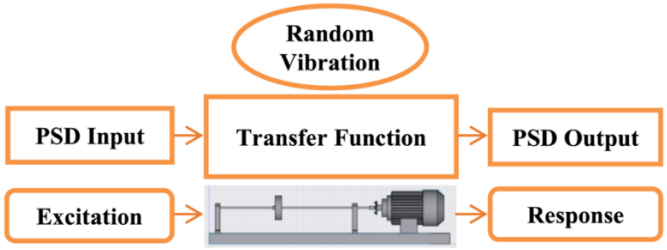

Fig. 5 Random Vibration Analysis.

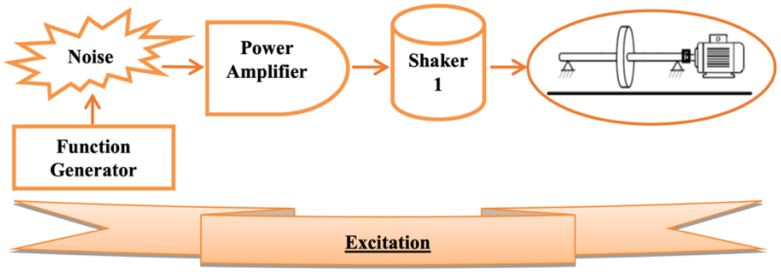

Fig. 6 Excitation Random Vibration.

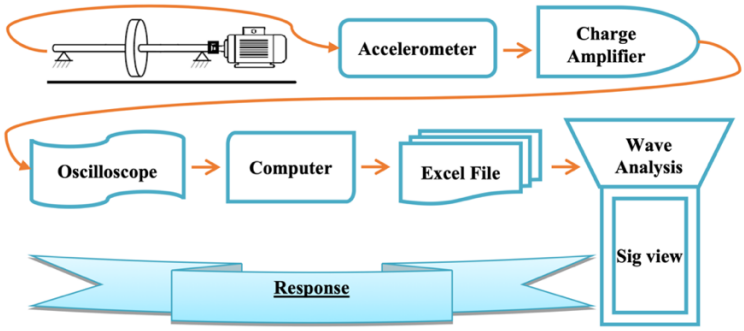

Fig. 7 Random Vibration Response.

Fig. 8 (a): Nanoparticles Mixed with Oil, (b): Using an Ultrasonic Bath to Lubricate Samples of Various Weights, (c): Viscosity Calculated Using a Viscometer Device.

The rotor's supports were lubricated with nanoparticle-enhanced oil, and the rotor was spun at 1000 rpm. A white noise generator and a power amplifier were utilized to move the shaker to produce a random vibration on the support. An oscilloscope was then used to view the waves after receiving vibration through an accelerometer and signal amplifier. The signal was then uploaded to the computer as an Excel file and analyzed, and the PSD could be determined using the SigView software.

To identify natural frequency and assess Gaussian distribution and probability, two separate waves were examined using the SigView application (Fig. 9). They were then converted into Fast Fourier transform (FFT) and PSD formats. The study investigated the relationship between journal-bearing lubrication and rotational speeds and nano-concentrations.

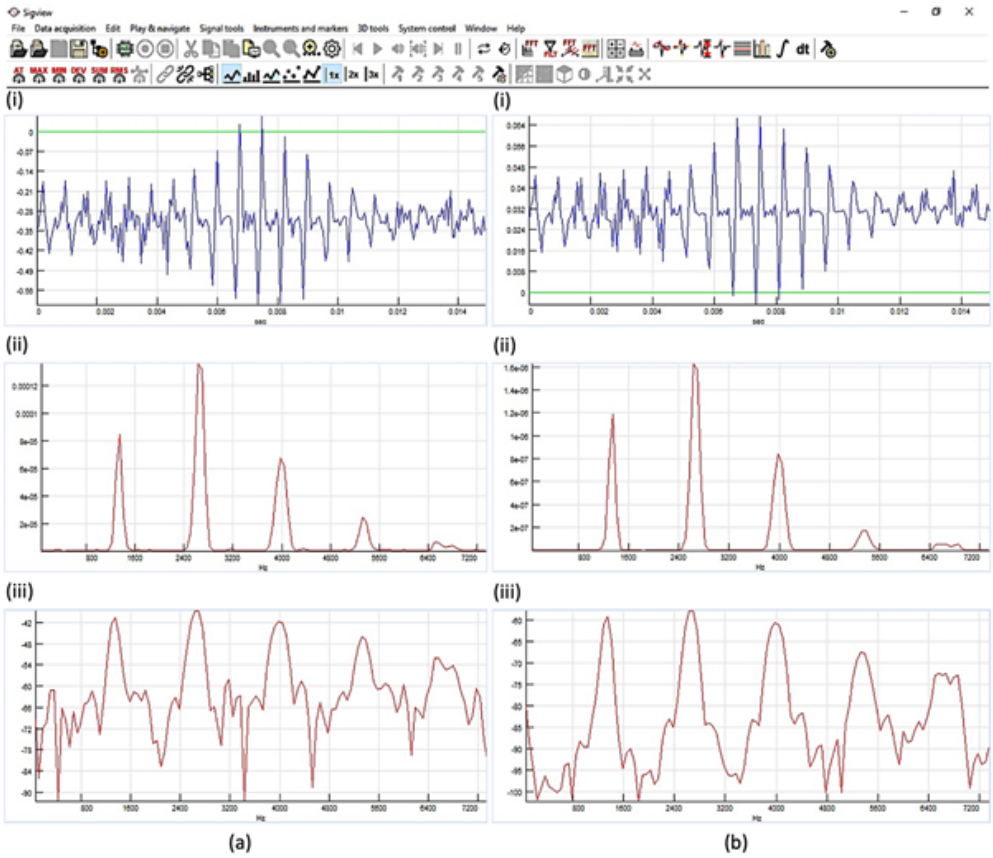

Fig. 9 SigView Software was Used to Analyze the Random Vibration Waves. (a) Waves are Presented as (i) Excitation Signal (Wave Signal (White Noise)), (ii) FFT, and (iii) PSD; and (b) Response Waves are Presented as (i) Response Signal (Wave Signal (White Noise)), (ii) FFT, and (iii) PSD.

4.RESULTS AND DISCUSSION

The impact of adding different CuO-NP concentrations to the oil lubricant is shown in Fig. 10. Because of how nanoparticles behave at different concentrations, both curves for two degrees of temperature showed that adding even a small concentration of nanoparticles increased the viscosity. However, as the concentration of CuO-NPs increased to 0.6g, the curves started to drop again. Similar studies reported a drop in viscosity with increasing the nanoparticle concentration [10,12]. The viscosity calculated for each sample of oils is also given (Table 2). The relationship between the power spectral density response at 1000 RPM and the frequency range of 0-90 rad/s is shown in Fig. 11. For comparison purposes, the first case represents the response of pure oil at a viscosity of 0.0507 Pa.s (without CuO-NP).

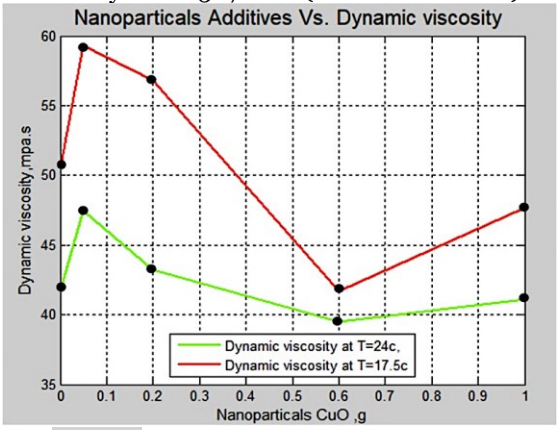

Fig. 10 Effects of Nanoparticles on Oil Viscosity.

Table 2 Characteristics of the Prepared CuO-NP-Enhanced Oil Samples.

Type of Sample	RPM	Temperature	Viscosity	Density
SAE 10w-30	100	17.5 °C	50.7 mPa.s	909.2 Kg/m^3
SAE 10w-30 with 0.0527 g of CuO-NP	100	17.5 °C	59.3 mPa.s	911.4 Kg/m^3
SAE 10w-30 with 0.2g of CuO-NP	100	17.5 °C	56.8 mPa.s	982.8 Kg/m^3
SAE 10w-30 with 0.6g of CuO-NP	100	17.5 °C	41.7 mPa.s	1055 Kg/m^3
SAE 10w-30 with 1 g of CuO-NP	100	17.5 °C	47.7 mPa.s	1125.8 Kg/m^3

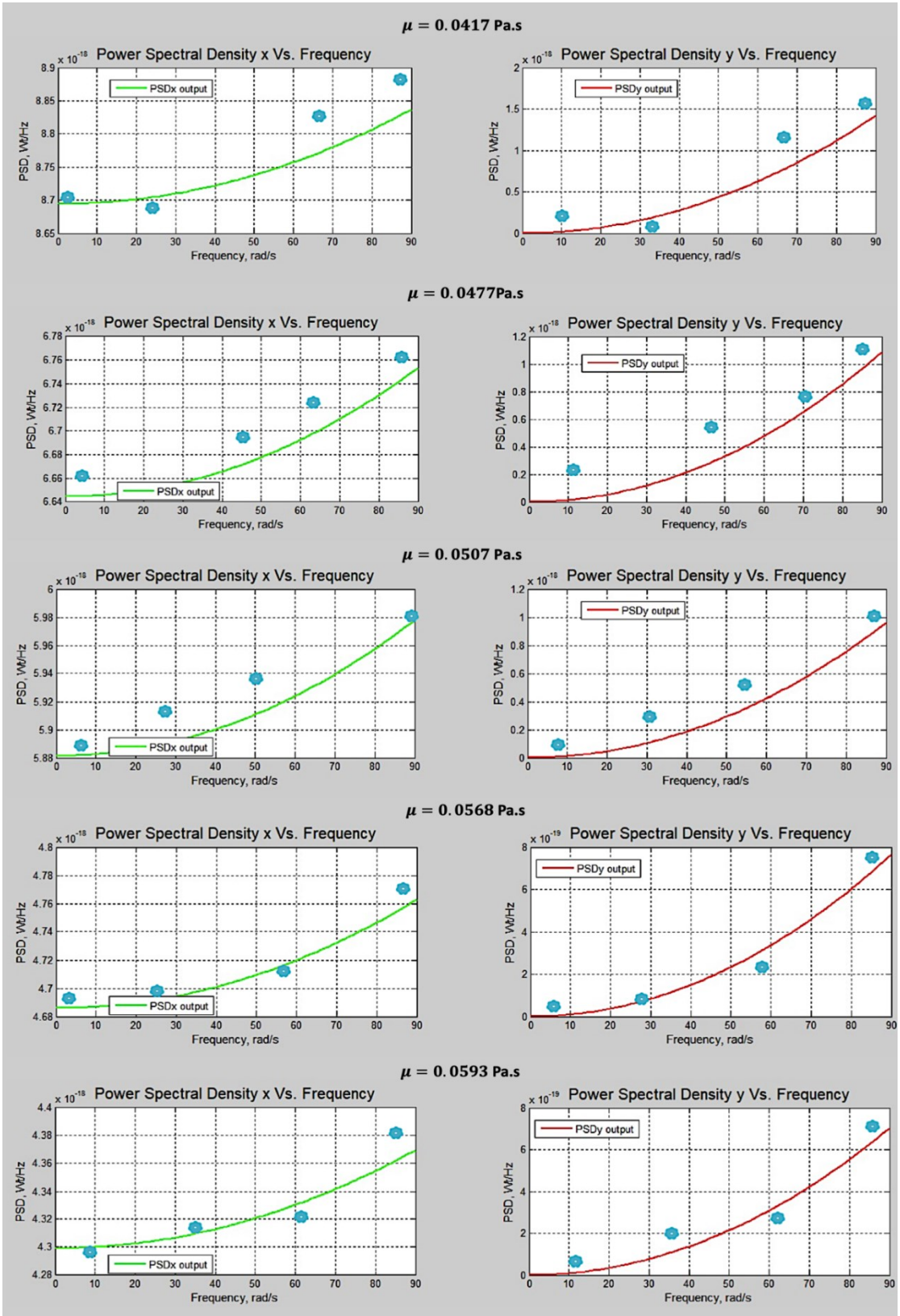

Fig. 11 PSD vs. Dynamic Viscosity (the Experimental Findings are Represented by the Blue Points).

The relationship between the transfer function and the dynamic viscosity is shown in Figs. 12-16. The lowest value of the real and imaginary transfer function (TF) in the x direction for all cases was at a viscosity of 0.0417 Pa.s. For the y direction, the lowest value for the real and imaginary was at 0.0417 Pa.s, except for the imaginary transfer function value in the y direction, which increased with increasing frequency.

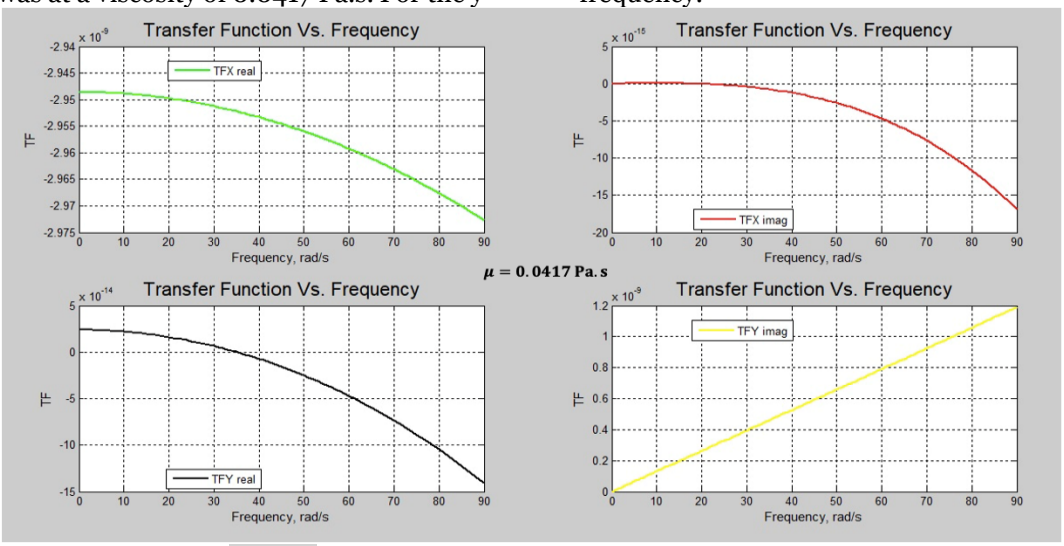

Fig. 12 TF vs. Dynamic Viscosity at μ= 0.0417 Pa.s.

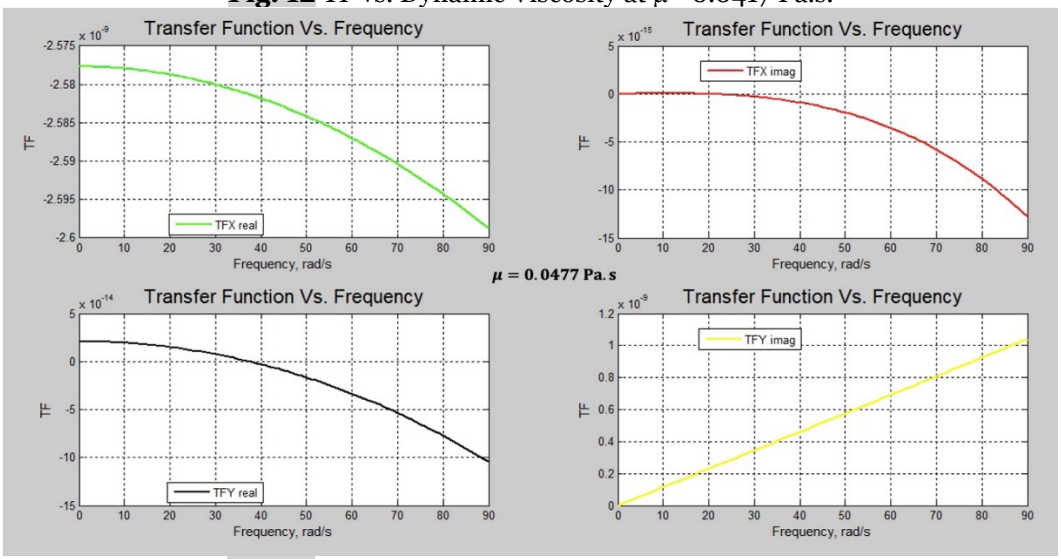

Fig. 13 TF vs. Dynamic Viscosity at μ= 0.0477 Pa.s.

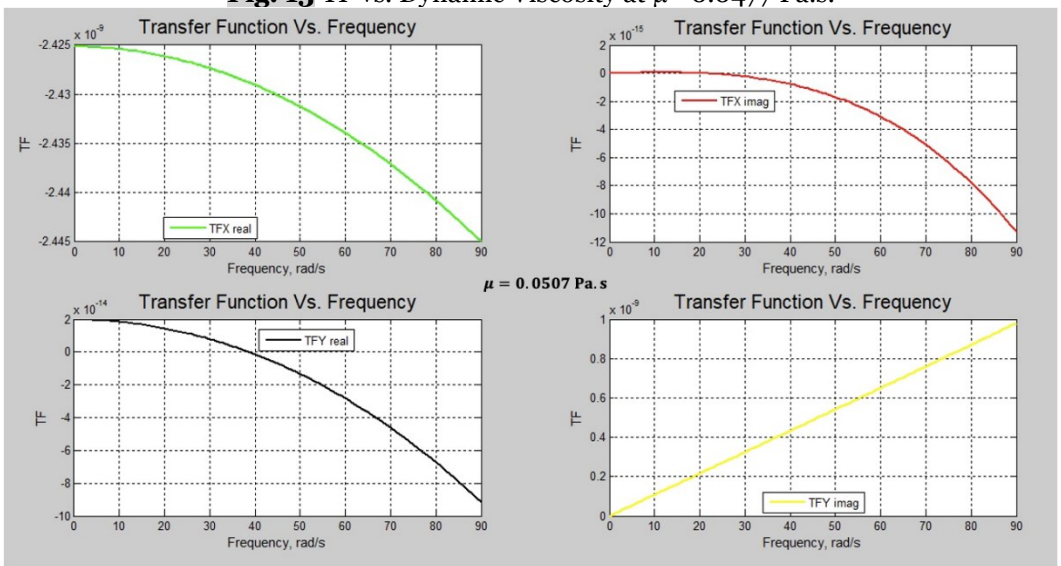

Fig. 14 TF vs. Dynamic Viscosity at μ= 0.0507 Pa.s.

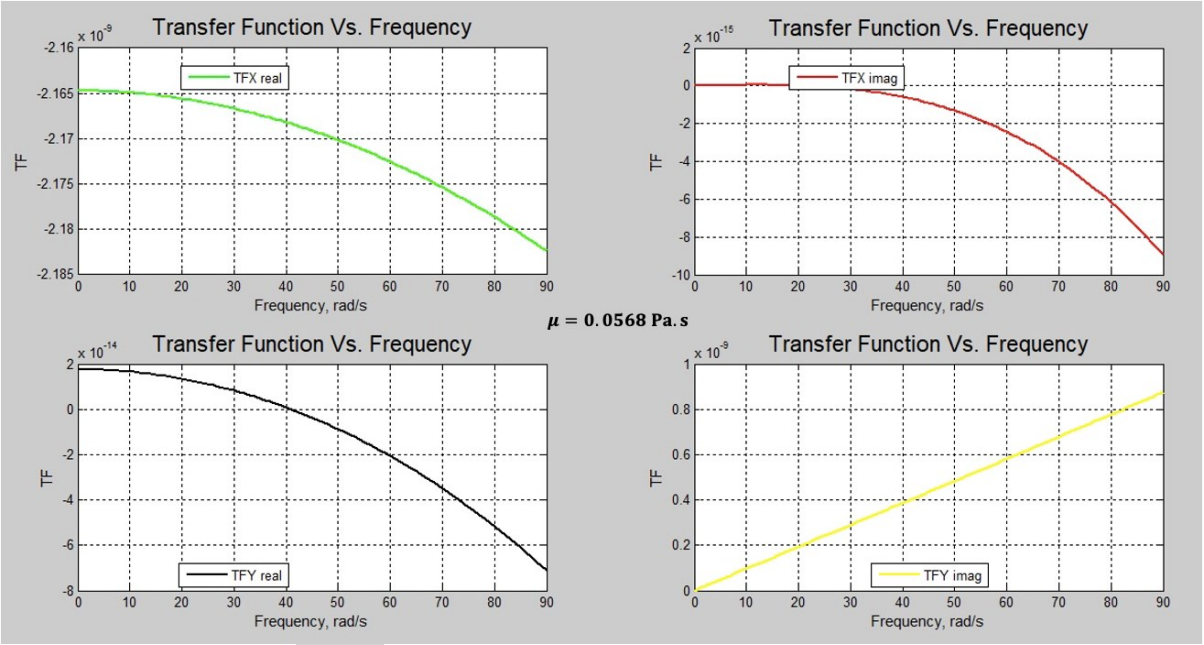

Fig. 15 TF vs. Dynamic Viscosity at μ= 0.0568 Pa.s.

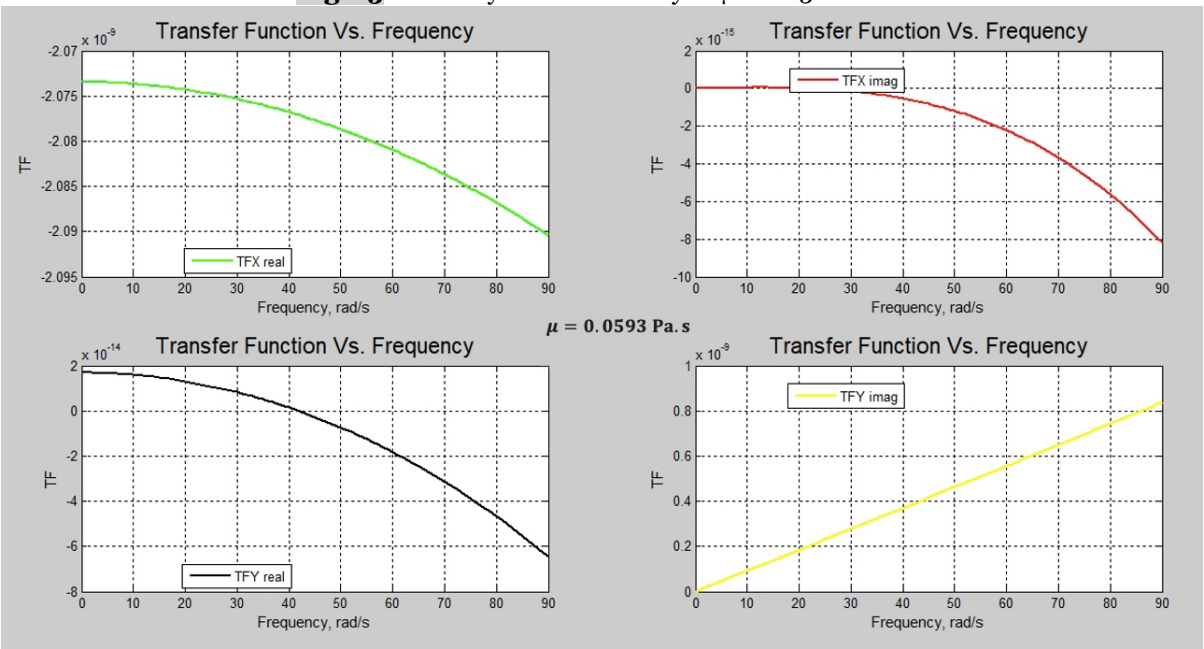

Fig. 16 TF vs. Dynamic Viscosity at μ= 0.0593 Pa.s.

The relationship between the standard deviation and the dynamic viscosity at different CuO-NPs is shown in Fig. 17. Assuming the random vibration is of a Gaussian distribution, it was discovered that at x = 2.249 and y=5.7522, the probability that the response in the x-direction was 68.3%, while at x = 4.498 and y = 11.14, the probability increased to 95.6%, and at x = 6.747 and y = 16.716, the probability reached 99.7% at 0.0507 Pa.s.

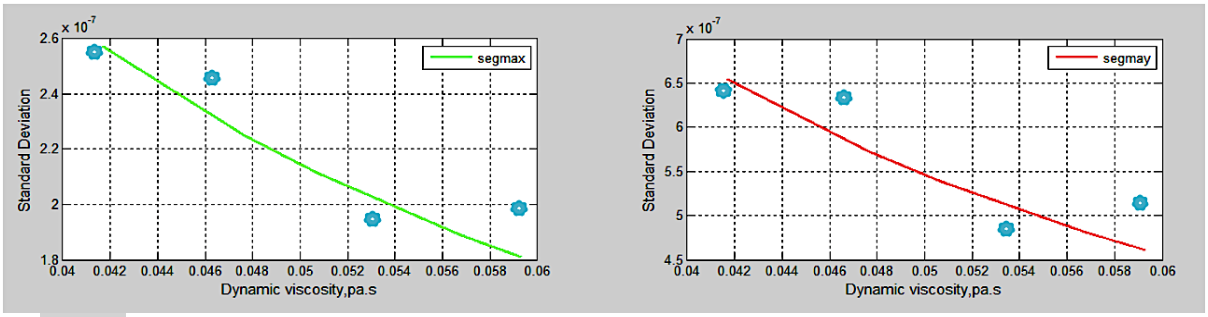

Fig. 17 Standard Deviation Vs. Dynamic Viscosity (The Blue Points Represent the Experimental Results).

The relationship between the standard deviation in the x and y directions at rotational speeds ranging from 900 to 3360 RPM is shown in Fig. 18. At 900 RPM, the standard deviation in the x and y directions was at its highest value. It then sharply dropped at 1500 RPM, decreased gradually until 2700 RPM, and stabilized horizontally until the highest rotor speed (3360 RPM) was reached. The standard deviation (σ) measures the asymmetry of the probability distribution. A decrease in standard deviation, observed in the x and y directions of the rotor system (from 3.289×10^{-7} to 2.812×10^{-7} and from 9.345×10^{-7} to 7.99×10^{-7}), indicated a shift toward a more symmetric distribution after lubrication with oil supplemented with 0.0527g CuO-NPs. Such a decrease in standard deviation indicates a more symmetric distribution of responses in the used rotor system after lubrication. A more symmetric distribution of forces or vibrations is desirable for improved performance and reduced wear in the rotor system. Sigma here represents the limits of response, and it decreases with increasing speed. These results showed that the critical speed had lower values with increasing rotational speeds.

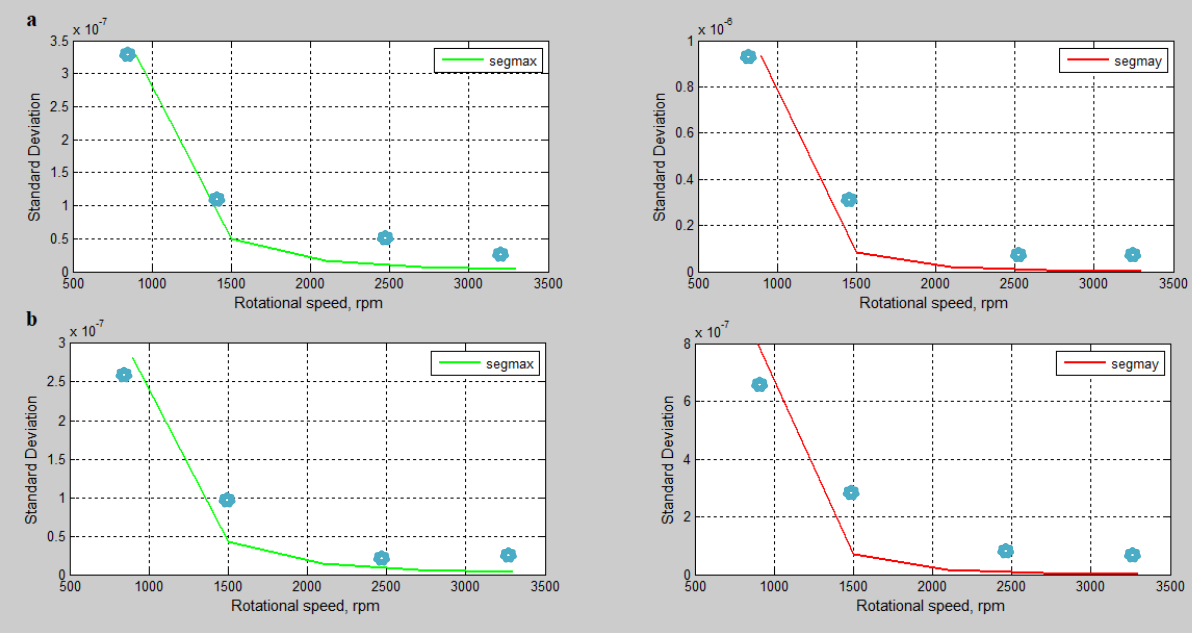

Fig. 18 Standard Deviation vs. Rotational Speed. (a) Normal Oil Viscosity = 0.0507 Pa.s. (b) Oil Supplemented with the Minimum NP Concentration with a Viscosity of 0.0593 Pa.s.

From the normal distribution using Eq. (28), it is concluded that the c of exceeding the specified displacement are [17]:

$$p[|X_c| > 3.289 * 10^{-7}] = 31.7\%$$
$$p[|Y_c| > 9.345 * 10^{-7}] = 31.7\%$$

and at 3 sigma:

$$p[|X_c| > 9.867 * 10^{-7}] = 0.3\%$$
$$p[|Y_c| > 28.035 * 10^{-7}] = 0.3\%$$

The Gaussian distribution chart (Fig. 19) shows the positive and negative values of the instantaneous response. To find the probability of the peak of the response from Rayleigh distribution Eq. (29):

$$p\left[X_{c\,peak} > 3.289 * 10^{-7}\right] = 60.7\%$$

$$p\left[Y_{c\,peak} > 9.345 * 10^{-7}\right] = 60.7\%$$

and at 3 sigma:

$$p\left[X_{c\,peak} > 9.867 * 10^{-7}\right] = 1.2\%$$

$$p\left[Y_{c\,peak} > 28.035 * 10^{-7}\right] = 1.2\%$$

Rayleigh distributions (Fig. 20) give only the positive and highest values, which are the absolute values of the mean of the peak. The percentages of 31.7 % and 0.3 % for sigma (1σ) and sigma (3σ), respectively, for the normal distribution and 60.7 % and 1.2 % for sigma (1σ) and sigma (3σ), respectively, for the Rayleigh distribution indicate the system's typical behavior.

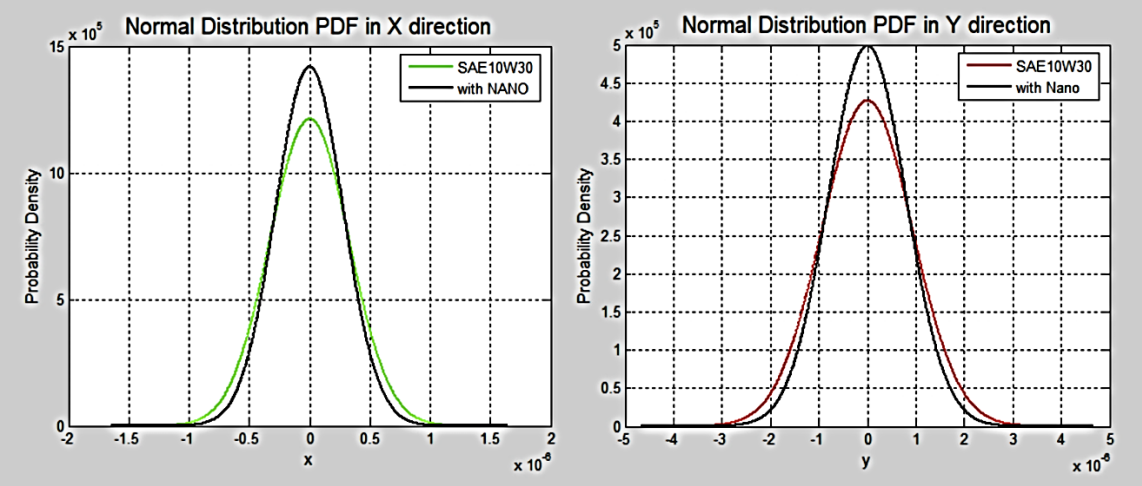

Fig. 19 Normal Distribution of Random Response in x and y Directions.

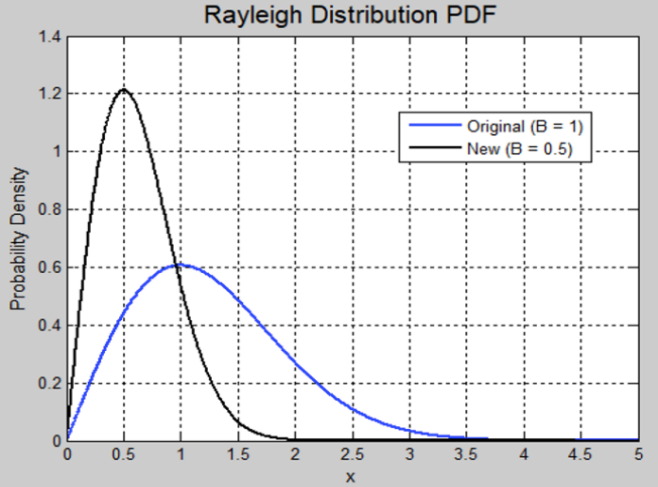

Fig. 20 Rayleigh Distribution of Random Response in x and y Direction.

60.7% represent the existence of less or secure amplitude. It is better in the case of a decreased standard deviation; thus, stress on the rotor is less, and the system becomes safer. In the case of high sigma, the opposite can occur and lead to failure. The relationship between the standard deviation and the distribution width is inversely proportional. A distribution more concentrated is indicated by a smaller standard deviation, whereas a higher standard deviation suggests a wider distribution, reducing noise or standard deviation closer to the mean, and enhances the probability of low amplitude, minimizing vibration-related issues in future system design. Beyond three sigma, the values become potentially riskier, signifying an even more extreme range. The analysis suggests that lubrication with oil supplemented with CuO-NPs positively impacted the rotor system, promoting a more symmetric distribution and thereby contributing to enhanced performance and safety.

5. CONCLUSIONS

The main conclusions are:

1- The mathematical model's results were reliable for analyzing the rotor's behavior with CuO nanoparticles.
2- The Jeffcott rotor model was used to derive complex transfer functions for system response to vibrations.
3- Experimental results showed improved dynamic viscosity with nanolubricants, reducing random vibration effects in the x and y directions.
4- Critical evaluations showed CuO-NPs positively impact critical speeds and displacement thresholds.
5- Oil quality improved by 14.5% with CuO-NPs, modifying the Gaussian distribution curve.
6- Theoretical and experimental results validated the effectiveness of 0.0527g CuO-NPs with 0.0593 Pa.s viscosity as optimal nano-additives for lubricants.
7- The noteworthy agreement between theoretical and experimental results for PSD random responses, with the largest error being 6.5%, confirms the model's reliability.
8- Transfer function analysis revealed characteristics enhanced in the x and y directions.

9- Rotor rotation speed affected the response standard deviation, with the highest value at 900 rpm.

10- The study provides a comprehensive understanding of rotor system dynamics under CuO-NP lubrication, with implications for theoretical understanding and practical applications in rotor system design and optimization.

ACKNOWLEDGMENTS

The authors would like to thank the employees at the Solar Energy Laboratory, the Nano Renewable Energy Research Center, mechanical engineering department and the chemical engineering department for their suggestions and help in creating nano-enhanced lubricants. Grant (PGRG) No.NU.G/2021/HIR/MOHE/ENG/(2674-111-1).

NOMENCLATURE

F_n	External force
c_{nx}	Rotating damping in x-direction
c_{ny}	Rotating damping in y-direction
F_x	Force in x-direction
$\Omega = N$	Spin speed, RPM.
m	Mass of the disc.
c_n	Rotating damping.
c_r	Non-rotating damping.
k_x	Real stiffness coefficient of the bearing in x direction, Ns/m.
k_y	Real stiffness coefficient of the bearing in x direction, Ns/m.
c_x	Real damping coefficient of the bearing in x direction, Ns/m.
c_y	Real damping coefficient of the bearing in y direction, Ns/m.
ω	Frequency, rad/s.
ω_{cr}	Critical speed, RPM.
c_y	Real damping coefficient of the bearing in y direction, Ns/m.

REFERENCES

[1] Mendes RU, Cavalca KL. **On the Instability Threshold of Journal Bearing Supported Rotors.** *International Journal of Rotating Machinery* 2014; **6**(2):1-7.

[2] Al-Wedyan HM, Tahat MS, Mutasher SA. **The Behaviour of the Jeffcott Rotor under a Vibrating Base of Fluid Film Bearing.** *Journal of Science and Technology* 2008; **15**(3): 167-176.

[3] Dimentberg MF, Naess A, Sperling L. **Response of a Rotating Shaft to Uniaxial Random Excitation.** *Journal of Sound and Vibration* 2012; **79**: 044503.

[4] Dimentberg MF, Ryzhik B, Sperling L. **Random Vibrations of a Damped Rotating Shaft.** *Journal of Sound and Vibration* 2005; **279**:275-284.

[5] Driot N, Berlioz A, Lamarque CH. **Stability and Stationary Response of a Skew Jeffcott Rotor With Geometric Uncertainty.** *Journal of Vibration and Acoustics* 2009; **4**(2): hal-02194284.

[6] Zapomel J, Ferfecki P, Kozánek J. **Effect of the Controllable Support Elements Lubricated by Magnetically Sensitive Fluids on Chaotic and Regular Vibration of Flexible Rotors During Rubbing.** *Mechanism and Machine Theory* 2021; **155**:104096.

[7] Yaroshevich N, Grabovets V, Yaroshevich T, Pavlova I, Bandura I. **On the Effect of Vibrational Capture of Rotation of an Unbalanced Rotor.** *Mathematical Models in Engineering* 2023; **9**(2):81-93.

[8] Asnida M, Hisham S, Awang NW, Amirruddin AK, Noor MM, Kadirgama K, Ramasamy D, Najafi G, Tarlochan F. **Copper (II) Oxide Nanoparticles as Additive in Engine Oil to Increase the Durability of Piston-Liner Contact.** *Fuel* 2018; **212**:656-667.

[9] Asrul M, Zulkifli NWM, Masjuki HH, Kalam MA. **Tribological Properties and Lubricant Mechanism of Nanoparticle in Engine Oil.** *Procedia Engineering* 2013; **68**:320-325.

[10] Thottackkad MV, Perikinalil RK, Kumarapillai PN. **Experimental Evaluation on the Tribological Properties of Coconut Oil by the Addition of CuO Nanoparticles.** *International Journal of Precision Engineering and Manufacturing* 2012; **13**:111-116.

[11] Jamalabadi MYA. **Effects of Nanoparticle Enhanced Lubricant Films in Dynamic Properties of Plain Journal Bearings at High Reynolds Numbers.** *International Journal of Engineering and Technology* 2017; **13**:1-23.

[12] Kumar M, Afzal A, Ramis MK. **Investigation of Physicochemical and Tribological Properties of TiO2 Nano-Lubricant Oil of Different Concentrations.** *Tribology Journal* 2017; **35**:6-15.

[13] Hammza TM, Abdulkareem AA, Abas EN. **Influence of the Solid Particles Nanofluid on the Dynamic Behaviour of Rotor Fluid Film Journal Bearing Systems.** *Journal of Mechanical Engineering Research and Development* 2020; **43**(7):149-162.

[14] Singh A, Verma N, Chaurasia A, Kumar A. **Effect of TiO2 Additive Volume Fraction in Lubricant Oil on the Performance of Hydrodynamic Journal Bearing.** *IOP Conference Series: Materials Science and Engineering* 2020; **802**(1):012005.

[15] Jaffar SS, Soud WA, Baqer IA. **A Comparative Study between Two Lubrication Nano-Additives (Bi2O3**

& TiO2) Based on Vibration Response Analysis. *Engineering and Technology Journal* 2023; **41**(1):60-68.

[16] Genta G. **Dynamics of Rotating Systems.** *Springer Science & Business Media* 2005.

[17] Thomson WT. **Theory of Vibration With Applications.** *Springer* 1993.